Comprehensive Characterization and Biological Assessment of a Newly Synthesized Adenine Derivative via Spectroscopy and DFT Approaches

Gana Saraswathy D. and Vijaya P.*
Rani Anna Government College for Women, Affiliated to Manonmaniam Sundaranar University, Tirunelveli, 627 012, INDIA
*auvijaya58@gmail.com

Abstract

4-((E)-(7H-purin-6-ylimino)methyl)-3-ethoxyphenol (3 EA) was synthesized and characterized by UV, IR, ^{1}H NMR and ^{13}C NMR. The anticancer activity was evaluated through a cell viability assay (MTT assay) performed on two cell lines: Caco2 (Human colorectal cancer cell) and A549 (Human lung cancer cell line). The conformational analysis of 3EA was performed by Density Functional Theory (DFT) methods using 6-31 G (d, p) basis set by Gaussian 03 program. The IR frequencies were analysed by means of potential energy distribution (PED%) calculation using the vibrational energy distribution analysis (VEDA[4]) program. The theoretical IR vibrational frequencies and UV-Vis spectrum were found to be in good agreement with experimental values.

The experimental NMR chemical shift values were compared with the theoretical values obtained by the DFT method. The stability of the molecule has been analysed using Natural Bond Orbital (NBO) analysis. The Schiff base 3EA was successfully synthesized, structurally characterized and its theoretical studies closely matched experimental results, confirming its stability and potential anticancer activity. NBO analysis, UV-Vis, IR and NMR data strongly support the molecule's conformational and electronic properties.

Keywords: DFT, UV-Vis, IR, NMR, NBO analysis, Anticancer activity, Caco2, A549, MTT assay.

Introduction

Adenine, one of the essential aromatic bases in the nucleic acids DNA and RNA, plays a fundamental role in the storage and transfer of genetic information. Derivatives of adenine have attracted considerable attention in recent years due to their diverse applications in medicine, biochemistry and molecular biology. Notably, their antiviral, antibacterial and anticancer properties have established adenine derivatives as promising candidates in therapeutic research. Parallelly, 2-ethoxy-4-hydroxybenzaldehyde, a functionalized benzaldehyde, is known for its significant biological activities including antimicrobial and antioxidant effects attributed to its reactive chemical structure. Motivated by the complementary properties of these two bioactive units, the present study focuses on the synthesis of a novel Schiff base, 4-((E)- (7H-purin-6-ylimino) methyl)- 3-ethoxyphenol (3EA).

The objective is to comprehensively investigate the synthesis, spectroscopic characterization (UV-Vis, IR, ^{1}H and ^{13}C NMR), theoretical properties using Density Functional Theory (DFT)[6] and biological activity through MTT assays against $CaCO_2$ and A549 cancer cell lines. The findings of this work are expected to contribute to drug development efforts and to enhance the understanding of the structural and biological behavior of adenine-based derivatives.

Material and Methods

All chemicals and reagents were obtained from Sigma-Aldrich and Loba Chemie and used without further purification. The FT-IR spectra of the synthesized compound 3EA were recorded in the range of 400–4000 cm^{-1} using the KBr pellet method. For UV-Visible analysis, the spectrum of 3EA was recorded on a UV-Vis Double Beam Touch Screen Spectrometer (Model LI-2900) using ethanol as the solvent at ambient room temperature, with the scan range set between 100–1100 nm. Proton (^{1}H) NMR spectra were recorded on a Bruker 400 MHz NMR spectrometer using dimethyl sulfoxide (DMSO) as the solvent.

Similarly, carbon (^{13}C) NMR spectra were recorded on a Bruker spectrometer at 100 MHz, also employing DMSO as the solvent. All cancer cell lines were procured from the National Centre for Cell Science (NCCS), Pune, India. The cytotoxicity evaluation experiments were conducted and analyzed by Athmic Biotech Solutions Pvt. Ltd., Thiruvananthapuram, India. In this study, the MTT assay was employed to measure cellular metabolic activity as an indicator of cytotoxicity.

Synthesis of 3EA: A mixture of adenine (0.001 mol, 0.1351 g), 2-ethoxy-4-hydroxybenzaldehyde (0.001 mol, 0.2833 g) and potassium hydroxide (0.1 mg) was dissolved in ethanol and placed in a 250 ml round-bottom (RB) flask. The reaction mixture was refluxed at 60 °C for 90 minutes under a water condenser until the solution changed to a dark red-orange color. The progress of the reaction was monitored by thin-layer chromatography (TLC) using a 1:1 (benzene: petroleum ether) solvent system. After completion, the reaction mixture was allowed to dry for 12 hours and the crude product was recrystallized from ethanol. The resulting yellow crystalline solid was obtained in 81% yield and subsequently used for further spectral characterization.

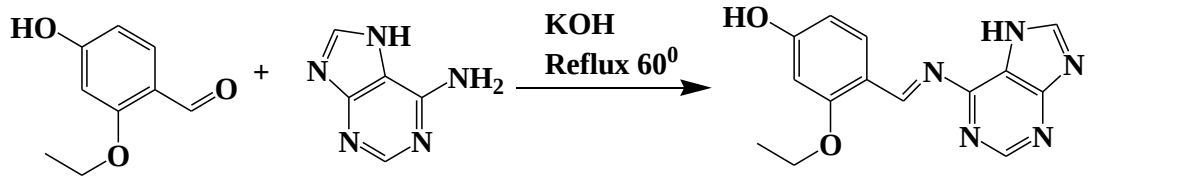

2-ethoxy-4-hydroxybenzaldehyde **Adenine** **4-((*E*)-(7*H*-purin-6-ylimino)methyl)-3-ethoxyphenol**

Scheme 1: Preparation of 4-((E)-(7H-purin-6-ylimino)methyl)-3-ethoxyphenol (3EA)

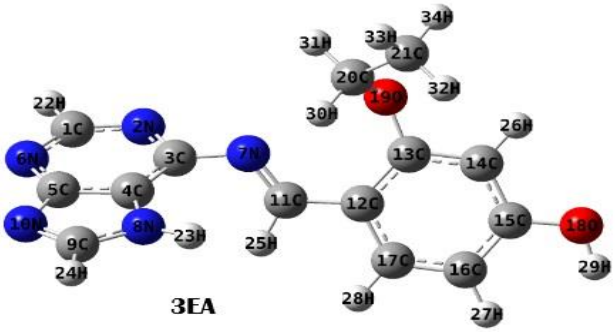

Figure 1: Optimized structure of 3EA.

Computational techniques: Density functional theory (DFT) calculations were performed using the Gaussian 03W program package with the B3LYP/6-31G (d,p) basis set. The 3EA molecule was designed and optimized to obtain its minimum energy conformer. Ultraviolet-visible (UV-Vis) spectroscopic analysis was conducted via Time-Dependent Self-Consistent Field (TD-SCF) calculations, employing ethanol as the solvent. Vibrational analysis was carried out on the optimized structure using the same basis set, applying a scaling factor of 0.9614 to correct the theoretical frequencies. The potential energy distribution (PED) of the molecule was analyzed using the VEDA[4] program. Furthermore, NMR calculations were performed using the 6-311+G (2d, p) basis set with DMSO as the solvent, applying scaling factors of 181.6032 for ^{13}C and 31.7838 for ^{1}H chemical shifts[16].

Spectral measurement: 4-((E)-(7H-purin-6-ylimino) methyl)-3-ethoxyphenol (3EA) ($C_{14}H_{13}N_5O_2$), Yield-81%,Colour-Pale yellow solid; UV-VIS absorbance (Ethanol, nm)-286,330,FT-IR (KBr, cm^{-1}) 3355 (phenolic –OH), 2981.00, 2801.00, 2695.00, 2600.00 (aromatic C–H), 1630.00, 1598.00 (C=N), 1444, 1417,1350 (aromatic C–N, C–C, bending and twisting), 1383, 1307, 1251 (aliphatic C-C-H bending);^{13}C NMR (100 MHz, DMSO-d_6, ppm) – 166.81 (C-OH phenolic carbon), 154.66, 152.22, 149.74, 141.31, 128.83, 117.24, 115.87, 111.11 (heteroaromatic C),63.52 (CH_2–O),15.21 (aliphatic CH_3).^{1}H NMR (400 MHz, DMSO-d_6, ppm) – 9.45 (aromatic -NH), 8.54, 8.09, 7.20, 7.10, 6.57 (heteraromatic H), 7.27 (imine), 3.98–3.93 (CH_2–O), 1.31–1.28 (aliphatic CH_3),Elemental analysis (%) –Calculated: (C – 59.4, H – 4.63, N – 24.7, O – 11.3), Experimental: (C – 60.07, H – 4.97, N – 23.56, O – 11.25).

Results and Discussion

Geometry optimization of 3EA: The compounds 3EA is theoretically constructed and optimized with basis set DFT/B3LYP- 6-31G (d,p)[7,11]. The compound 3EA has 34 atoms and 148 electrons with C1 point group. Numbering for the optimized structure for 3EA is shown in fig.1. The heat of formation value of the compound is -965.51925448 a.u.

FT-IR computation of 3EA: The molecule 3EA consists of 34 atoms and hence 96 normal modes of vibrations and the molecule belongs to C1 symmetry [3]. All the modes are IR active. The theoretical vibrational spectra of 3EA have been calculated using DFT method with 6-31 G (d,p) basis set. The calculated IR frequencies are scaled by a factor 0.9614. In addition, theoretical IR vibrational spectra are interpreted by potential energy distribution (PED%) calculation using vibrational energy distribution (VEDA[4]) program [5]. The normal modes assignment of the theoretical IR frequencies is pictured and validated with Gauss view 5.0 program. The normal modes are given in order of decreasing wavenumber in table 1. None of the calculated vibrational frequencies have any negative frequencies, showing that the optimized structures are located at the ground state energy. The experimental and theoretical spectra of the molecules 3EA are picturized in fig. 2.

The IR spectral analysis of 3EA shows a strong O–H stretching band at 3355 cm^{-1} (theoretical 3669 cm^{-1}) and an N–H stretching band at 3308 cm^{-1} (theoretical 3531 cm^{-1}), confirming the presence of hydroxyl and amine groups. C–H stretching vibrations [13] were observed between 2981–2801 cm^{-1}, matching theoretical frequencies (3059–3023 cm^{-1}), indicating the structural integrity of aromatic and aliphatic systems. The characteristic C=N stretch appears at 1630 cm^{-1} (theoretical 1695 cm^{-1}), confirming successful Schiff base formation [20]. Aromatic and purine ring vibrations [4] were noted between 1598–1444 cm^{-1} while the C–O stretch appeared at 1307 cm^{-1} (theoretical 1297 cm^{-1}), supporting the phenolic structure. In-plane and torsional vibrations below 1400 cm^{-1}, along with low-frequency ring

deformations (1022–540 cm^{-1}), confirm the molecular flexibility and planarity. The close match between experimental and theoretical IR spectra verifies the successful synthesis and structural integrity of the 3EA compound.

UV-Vis analysis of 3EA: The compound 3EA is analysed using a UV-Vis spectrophotometer with ethanol as solvent [2,15]. The experimental and the theoretical absorbance for 3EA are illustrated in fig. 3 and respective energy contributions are tabulated in table 2. In the UV-Vis spectrum of 3EA, two main absorption bands are observed at 330 nm and 286 nm, corresponding to $\pi \rightarrow \pi^*$ and mixed $\pi \rightarrow \pi^*/n \rightarrow \pi^*$ transitions within the conjugated system, involving the imine linkage and aromatic moieties. TD-DFT calculations (scrf = solvent: ethanol) predict absorption bands at 319 nm, 294 nm and 282 nm, closely matching the experimental results and validating the theoretical model. The major transitions are assigned to HOMO → LUMO, H-1 → LUMO and H-2 → LUMO, predominantly $\pi \rightarrow \pi^*$ in nature, indicating strong delocalization across the adenine and benzaldehyde units.

Minor contributions from deeper orbitals (H-3, L+1, L+2) explain fine spectral features. The close agreement between experimental and theoretical data confirms an extended π-conjugated system, suggesting enhanced electronic communication, chemical reactivity and potential biological activities such as DNA binding or anticancer effects.

NMR analysis of 3EA: The theoretical ^{13}C and ^{1}H NMR spectrum of the compounds 3EA is computed with GIAO method[8] using the basis set B3LYP with 6–311-G + (2d,p) and TMS as reference [scrf = (solvent = DMSO)] and the isotropic values obtained in the calculations were subtracted from the scaling factor of 31.783 ppm and 181.6032 ppm to obtain the chemical shift for ^{1}H NMR and ^{13}C NMR respectively [17,18]. The theoretical and experimental chemical shift values of ^{1}H and ^{13}C NMR are tabulated in table 3. The experimental values of the compounds 3EA are in good agreement with computed chemical shifts values.

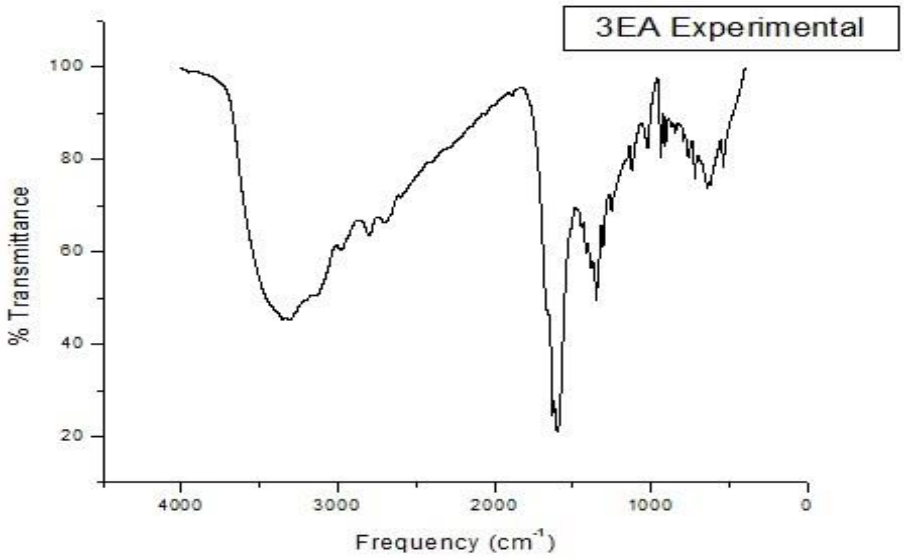

Figure 2: Experimental FT-IR spectrum of 3EA.

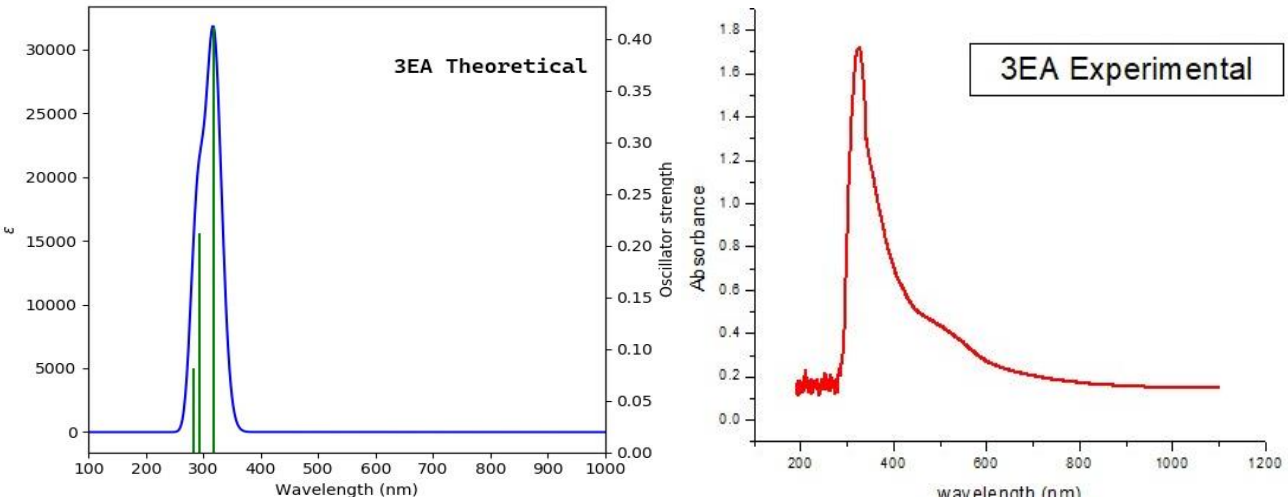

Figure 3: Theoretical and experimental absorbance of 3EA.

Table 1
Significant vibrational wavenumbers obtained for 3EA at B3LYP/6-31G (d,p) level of calculations

3EA				
Mode No.	**Theoretical frequencies (cm^{-1}) DFT/B3LYP/6-31G(d,p)**		**Observed frequencies (cm^{-1})**	**Vibrational assignment PED ≥20%**
	Unscaled frequencies	**Scaled frequency scaling factor = 0.9614**		
96	3817	3669	3355	ν $_{O18-H29}$ (100%)
95	3673	3531	3308	ν $_{N8-H23}$ (100%)
91	3182	3059	2981	ν $_{C1-H22}$ (100%)
89	3144	3023	2801	ν $_{C16-H27}$ (43%) + ν $_{C17-H28}$ (57%) +ν $_{C21-H32}$ (14%) + ν $_{C21-H34}$ (19%)
86	3078	2959	2695	ν $_{C20-H30}$ (72%) + ν $_{C20-H31}$ (25%)
84	3008	2892	2600	ν $_{C11-H25}$ (100%)
83	1764	1695	1630	ν $_{N7-C11}$ (78%)
82	1672	1607		ν $_{C14-C15}$ (16%) + ν $_{C17-C12}$ (15%)
81	1639	1576	1598	ν $_{N6-C1}$ (17%) + ν $_{N8-C4}$ (22%)
80	1612	1550		ν $_{C15-C16}$ (34%)
79	1597	1535		ν $_{N2-C3}$ (13%) + ν $_{N6-C5}$ (27%) + β $_{C4-N8-C9}$ (12%)
77	1531	1472	1444	ν $_{N10-C9}$ (36%) + β $_{H24-C9-N10}$ (14%)
75	1510	1451		ν $_{N2-C3}$ (10%) + β $_{H22-C1-N6}$(18%) + β $_{H22-C21-H34}$(19%)
72	1489	1432	1417	ν $_{C13-C14}$ (13%) + β $_{H31-C20-H30}$ (15%)
69	1411	1357		ν $_{N8-C9}$ (26%) + β $_{H23-N8-C9}$ (30%)
68	1398	1344	1383	β $_{H31-C20-H30}$ (14%) + τ $_{H30-C20-O19-C13}$ (16%) + τ $_{H31-C20-O19-C13}$ (28%)
67	1395	1341		ν $_{N6-C1}$ (10%) + ν $_{N8-C4}$ (30%) + β $_{C4-N8-C9}$ (12%) + β $_{H24-C9-N10}$ (13%)
66	1375	1322	1350	ν $_{C16-C17}$ (17%) + ν $_{C13-C14}$ (10%) + ν $_{C17-C12}$ (12%)
65	1368	1316		ν $_{N10-C5}$ (28%)
64	1350	1297	1307	ν $_{O18-C15}$ (26%)
63	1338	1287		ν $_{N2-C3}$ (12%) + β $_{H22-C1-N6}$ (16%)
62	1319	1268	1251	β $_{H30-C20-C21}$ (49%) + τ $_{H30-C20-O19-C13}$ (15%) + τ $_{H31-C20-O19-C13}$ (13%)
60	1276	1227		ν $_{N10-C9}$ (15%) + ν $_{N6-C1}$ (10%) + β $_{H24-C6-N10}$ (26%)
58	1247	1199	1123	ν $_{O19-C13}$ (13%) + ν $_{C12-C11}$ (10%) + β $_{H29-O18-C15}$ (15%)
57	1235	1187		ν $_{C12-C11}$ (17%) + β $_{H29-O18-C15}$ (20%)
56	1193	1147	1022	β $_{H30-C20-C21}$ (12%) + τ $_{H30-C20-O19-C13}$ (15%) + τ $_{H32-C21-C20-O19}$ (10%) + τ $_{H34-C21-C20-O19}$ (10%)
54	1185	1139	938	β $_{H29-O18-C15}$ (19%) + β $_{H26-C14-C15}$ (24%) + β $_{H27-C16-C17}$ (18%)
53	1154	1110	910	β $_{H27-C16-C17}$ (22%) + β $_{H87-C17-C18}$ (10%)
52	1112	1069	868	ν $_{N8-C9}$ (52%) + β $_{H23-N8-C9}$ (22%)
50	1072	1030	846	ν $_{N7-C3}$ (15%) + β $_{C4-N8-C9}$ (24%) + β $_{H23-N8-C9}$ (16%)
49	1049	1009		ν $_{C21-C20}$ (31%)
48	1010	971	795	τ $_{H25-C11-N7-C3}$ (79%)
43	896	861	762	ν $_{O19-C20}$ (15%) + τ $_{H26-C14-C15-C16}$ (24%)
42	886	852	721	β $_{N2-C1-N6}$ (28%) + β $_{C5-N10-C9}$ (17%)
22	474	456	540	β $_{C15-C16-C17}$ (18%) + β $_{O18-C15-C16}$ (13%) + β $_{O19-C13-C14}$ (26%)

ν –stretching vibration; β – bending vibration; τ – torsion;

Table 2
Absorbance and contributions of 3EA computed by B3LYP/6-31G(d,p) TD-SCF DFT method

Name	Energy (cm^{-1})	Wavelength (nm)		Major contributions	Minor contributions
		Experimental value	Theoretical value		
3EA	31357.2	330	319	H-1->LUMO (30%), HOMO->LUMO (58%)	-
	34026.9	286	294	H-1->LUMO (45%), HOMO->LUMO (26%)	H-3->LUMO (9%), H-2->LUMO (3%), HOMO->L+1 (7%)
	35447.3	-	282	H-2->LUMO (84%)	HOMO->L+2 (9%)

Table 3
^{1}H and ^{13}C NMR Chemical Shift for 3EA computed by B3LYP/6-311+G(2d,p) GIAO DFT method

3EA					
^{13}C NMR	Theoretical chemical shift values (ppm)	Experimental chemical shift values (ppm)	^{1}H NMR	Theoretical chemical shift values (ppm)	Experimental chemical shift values (ppm)
C15	169.80	166.81	H23	9.533	9.450
C5	169.22		H22	9.101	8.542
C11	168.87		H25	8.753	7.276
C13	168.74		H24	8.584	8.093
C3	165.44	154.66	H28	7.937	7.202
C1	159.27	152.22	H27	7.118	6.577
C9	150.79	149.74	H26	7.092	7.108
C17	145.95	141.31	H29	6.175	No peak
C12	125.62	128.83	H31	4.374	3.981-3.931
C4	120.03	117.24	H30	4.146	
C14	116.85	115.87	H32	1.392	1.318-1.284
C16	114.12	111.11	H34	1.323	
C20	75.40	63.52	H33	0.871	
C21	14.84	15.21			

The ^{13}C NMR analysis of 3EA shows high theoretical shifts (~169–168 ppm) for carbonyl and imine carbons (C15, C5, C11, C13)[10], consistent with strong de-shielding. Experimental values closely match, confirming Schiff base formation. Aromatic carbons (C3, C1, C9, C4) appear between 120–165 ppm, verifying the conjugated adenine ring structure. Aliphatic and ether carbons (C20, C21) show shift consistent with oxygen substitution and terminal methyl groups. The ^{1}H NMR spectrum shows aromatic and imine protons (H22, H23, H24, H25) between 9.4–8.0 ppm, confirming proximity to electronegative groups.

Aromatic protons (H26, H27) appear as expected, while the hydroxy proton (H29) is not observed, likely due to hydrogen bonding. Methylene (H30, H31) and methyl protons (H32–H34) are correctly positioned in downfield and upfield regions respectively. The close match between theoretical and experimental NMR data confirms the structural integrity and successful synthesis of the 3EA Schiff base.

NBO analysis of 3EA: The NBO (Natural Bond Orbital) analysis provides insights into the electronic structure, charge delocalization and stabilization energies of a molecule. The NBO analysis of the compounds 3EA is computed using B3LYP/ 6-31 G (d,p) basis set. The donor bonding orbital (BD) and acceptor antibonding orbital (BD*) and donor lone pair (LP) along with the E(2) value are given in table 4. The energy E(2) is known as stabilization energy, suggesting that larger is the E(2) value, greater will be the stability. The higher is the occupancy of a donor orbital, the more stable is the electron configuration. The lower is the occupancy of an acceptor orbital, the more available it is to accept electron density [12,19].

NBO analysis of 3EA reveals strong π-conjugation and delocalization, with significant stabilization energies from π(N2–C3) → π*(C1–N6) (31.27 kcal/mol) and π(C4–C5) → π*(N2–C3) (31.57 kcal/mol) transitions. The π(C9–N10) → π*(C4–C5) (21.08 kcal/mol) interaction further stabilizes the imine linkage. A highly strong lone pair delocalization from N8 → π*(C9–N10) (46.65 kcal/mol) and C12 → π*(C16–C17) (78.87 kcal/mol) enhances aromatic stabilization. Moderate σ → σ* interactions, like σ(C1–N2) → σ*(C3–N7) and σ(C3–N7) → σ*(C11–C12), along with charge transfer involving electronegative atoms (O, N), support overall molecular stability. Minor contributions from C20–C21 and O19–C20 bonds fine-tune the electron distribution. These interactions collectively confirm the strong resonance, hyperconjugation and electronic stability of the Schiff base framework.

Table 4
Second order perturbation theory analysis of fock matrix in NBO basis for 3EA

3EA				
Donor NBO (i)	**Occupancy**	**Acceptor NBO(j) BD***	**Occupancy**	**E(2) in kcal/mol**
(σ)C1-N2	1.99	(σ*)C3-N7	0.04	4.73
(π)C1-N6	1.87	(σ*)C5-N10	0.03	6.70
(π)N2-C3	1.85	(π*)C1-N6	0.18	31.27
(σ)C3-C4	1.98	(σ*)C4-C5	0.05	3.54
(σ)C3-N7	1.98	(σ*)C11-C12	0.03	4.61
(π)C4-C5	1.78	(π*)N2-C3	0.22	31.57
(σ)C4-N8	1.98	(σ*)C5-N6	0.03	3.19
(σ)C5-N6	1.98	(σ*)C4-C5	0.05	1.72
(σ)C5-N10	1.98	(σ*)C3-C4	0.05	2.61
(π)N7-C11	1.96	(π*)N2-C3	0.22	4.73
(σ)N8-C9	1.99	(σ*)C3-C4	0.05	5.86
(π)C9-N10	1.92	(π*)C4-C5	0.05	21.08
(σ)C11-C12	1.97	(σ*)C3-N7	0.04	4.08
(σ)C12-C13	1.97	(σ*)C12-C17	0.04	3.15
(σ)C12-C17	1.97	(σ*)C13-O19	0.03	4.12
(π)C13-C14	1.83	(σ*)C15-O18	0.02	3.40
(σ)C13-O19	1.99	(σ*)C14-C15	0.02	1.62
(σ)C14-C15	1.97	(σ*)C13-O19	0.03	3.43
(σ)C15-C16	1.98	(σ*)C14-C15	0.02	3.43
(σ)C15-O18	2.00	(σ*)C13-C14	0.02	1.44
(π)C16-C17	1.85	(σ*)C15-O18	0.02	4.34
(σ)O19-C20	1.97	(σ*)C13-C14	0.02	1.14
(σ)C20-C21	1.99	(σ*)C13-O19	0.03	0.74
(LP)N2	1.91	(σ*)C1-N6	0.03	12.39
(LP)N6	1.91	(σ*)C1-N6	0.03	12.78
(LP)N7	1.85	(π*)N2-C3	0.22	14.94
(LP)N8	1.62	(π*)C9-N10	0.16	46.65
(LP)N10	1.92	(σ*)N8-C9	0.04	9.95
(LP)C12	1.09	(π*)C16-C17	0.18	**78.87**
(LP)O18	1.98	(σ*)C15-C16	0.03	6.42
(LP)O19	1.94	(π*)C13-C14	0.18	10.58

Table 5
Percentage of viability for varying concentration of 3EA against Caco2 cell line and A549 cell line

Concentration (µg/ml)	**Percentage of viability of Caco2 cell line**	**Percentage of viability of A549 cell line**
6.25	98.28	99.72
12.5	94.74	98.02
25	87.38	94.55
50	75.01	92.52
100	64.80	88.75
IC 50	**>100 µg/ml**	**>100 µg/ml**

Anti-cancer activity by MTT assay of 3EA: Anti-cancer activity of the compound 3EA was studied by MTT assay[9] on two cancer cell line human cancer cells: Caco2 (Human colorectal cancer cell) [1] and A549 (Human lung cancer cell line). The anti-cancer activity of 3EA on the Caco2 cell line and A549 cell line is observed by measuring cell viability at different concentrations (Table 5). The cytotoxicity of the synthesized Schiff base 3EA was assessed against the Caco-2 human colorectal cancer cell line using the MTT assay across concentrations ranging from 6.25 to 100 µg/ml. Cell viability progressively decreased from 98.28% (6.25 µg/ml) to 64.80% (100 µg/ml), indicating a concentration-dependent cytotoxic effect. Moderate cytotoxicity was observed at 50 µg/mL (75.01%) and a more pronounced effect at 100 µg/ml. However, the IC_{50} value was determined to be greater than 100 µg/ml, suggesting that 3EA exhibits moderate to weak anticancer activity under the experimental conditions with limited potency against the Caco-2 cell line.

The cytotoxicity of the synthesized compound 3EA was evaluated against the A549 human lung carcinoma cell line[14]. High cell viability was maintained across all tested concentrations, ranging from 99.72% (6.25 µg/ml) to 88.75% (100 µg/ml), indicating only a mild, dose-dependent cytotoxic effect. The IC_{50} value exceeded 100 µg/ml, confirming weak anticancer activity against A549 cells. However, the low cytotoxicity profile suggests that 3EA could serve as a promising candidate for further structural optimization or as a component in combination therapies aimed at enhancing anticancer efficacy while minimizing toxicity to normal cells.

Summary

In this study, the Schiff base 4-((E)-(7H-purin-6-ylimino) methyl)-3-ethoxyphenol (3EA) was synthesized by reacting adenine with 2-ethoxy-4-hydroxybenzaldehyde and was characterized using UV-Vis, FT-IR, ^{1}H NMR and ^{13}C NMR spectroscopy. The UV-Vis spectrum exhibited two main absorption bands at 286 nm and 330 nm, corresponding to $\pi \rightarrow \pi^*$ and mixed $\pi \rightarrow \pi^*/n \rightarrow \pi^*$ transitions, which were well-supported by Time-Dependent Density Functional Theory (TD-DFT) calculations. The FT-IR spectrum showed a strong O–H stretch at 3355 cm^{-1}, N–H stretch at 3308 cm^{-1} and C=N stretch at 1630 cm^{-1}, confirming the Schiff base linkage.

Aromatic and aliphatic C–H stretches were observed between 2981–2801 cm^{-1}. The ^{1}H NMR spectrum indicated aromatic and imine protons between 9.4–6.6 ppm, while ^{13}C NMR showed characteristic shifts around 168–169 ppm for carbonyl and imine carbons. These results are in good agreement with the theoretical calculations. The anti-cancer activity of 3EA was evaluated against the Caco2 (human colorectal cancer) and A549 (human lung cancer) cell lines using the MTT assay. The compound demonstrated moderate cytotoxicity against Caco2 cells, with cell viability decreasing from 98.28% at 6.25 µg/ml to 64.80% at 100 µg/ml, although the IC_{50} value was greater than 100 µg/ml, indicating weak anticancer activity. In contrast, 3EA showed minimal cytotoxicity against A549 cells, with cell viability ranging from 99.72% to 88.75% across the tested concentrations, confirming only mild cytotoxic effects. The low cytotoxicity profile of 3EA suggests that while it has potential as an anticancer agent, further structural optimization is necessary to enhance its efficacy and potency in cancer therapy.

Acknowledgement

The authors are thankful to Rani Anna Government College for Women, Tirunelveli, for providing lab facilities.

References

1. Albratty M. and Alhazmi, H. A., Novel pyridine and pyrimidine derivatives as promising anticancer agents, A review, *Arabian Journal of Chemistry*, **15(6)**, 103846 **(2022)**

2. Bassey V.M., Agwupuye J.A., Emori W., Apebende C.G., Asogwa F.C., Cheng C.R., Louis H., Unimuke T.O., Wei K. and Idante P.S., Vibrational Characterization and Molecular Electronic Investigations of 2-acetyl-5-methylfuran using FT-IR, FT-Raman, UV-VIS, NMR and DFT Methods, *Journal of Fluorescence*, **32(3)**, 1005–1017 **(2022)**

3. Berden G., Zundel L.P. and Oomens J., IR spectroscopy of isolated neutral and protonated adenine and 9-methyladenine, *Chemical Physics Letters*, **510(1–3)**, 30–35 **(2011)**

4. Blomberg M.R.A., Siegbahn P.E.M. and Brehm G., Investigation of coordination properties of isolated adenine to copper, *Spectrochimica Acta Part A: Molecular and Biomolecular Spectroscopy*, **111**, 205–212 **(2013)**

5. Cataldo P.G., Alvarez L.G. and Murgich J., Vibrational assignments of cyclic dimers and inter-monomers of adenine relating FT-IR, FT-Raman and UV spectra with SQMFF and DFT calculations, *Spectrochimica Acta Part A: Molecular and Biomolecular Spectroscopy*, **308**, 123456 **(2023)**

6. Corregidor P.F., Zigolo M.A. and Ottavianelli E.E., Conformational search, structural analysis, vibrational properties, reactivity study and affinity towards DNA of the novel insecticide flonicamid, *Journal of Molecular Structure*, **1241**, 130628 **(2021)**.

7. Kanmazalp S.D., Macit M. and Dege N., Hirshfeld surface, crystal structure and spectroscopic characterization of (E)-4-(diethylamino)-2-((4-phenoxyphenylimino)methyl)phenol with DFT studies, *Journal of Molecular Structure*, **1179**, 181–191 **(2018)**

8. Legault P. and Pardi A., *In situ* probing of adenine protonation in RNA by ^{13}C NMR', Journal of the American Chemical Society, **116(18)**, 8390–8391 **(1994)**

9. Mosmann T., Rapid colorimetric assay for cellular growth and survival: application to proliferation and cytotoxicity assays, *Journal of Immunological Methods*, **65(1-2)**, 55-63 **(1983)**

10. Rinnenthal J. and Schwalbe H., HNHC: a triple resonance experiment for correlating the H2, N1(N3) and C2 resonances in adenine nucleobases of ^{13}C,^{15}N-labeled RNA oligonucleotides, *Journal of Biomolecular NMR*, **44(2)**, 101–105 **(2009)**

11. Sarala S., Geetha S.K., Asif F.B. and Muthu S., Vibrational spectra and Wavefunction investigation for antidepressant drug of Amoxapine based on quantum computational studies, *Chemical Data Collections*, **33**, 100699 **(2021)**

12. Sakr M.A.S., El-Etrawy A.A.S. and Sherbiny F.F., Hydrazone-based Materials; DFT, TD-DFT, NBO Analysis, Fukui Function, MESP Analysis and Solar Cell Applications, *Journal of Fluorescence*, **32(5)**, 1857–1871 **(2022)**

13. Seethalakshmi M. and Sundaraganesan N., Molecular structure and vibrational spectra of p-fluorobenzaldehyde by density functional theory calculations, *Journal of Molecular Structure*, **975(1-3)**, 365–370 **(2010)**

14. Tasneem S., Sheikh K.A., Naematullah M., Alam M.M., Khan F., Garg M. and Shaquiquzzaman M., Synthesis, biological evaluation and docking studies of methylene bearing cyanopyrimidine derivatives possessing a hydrazone moiety as potent Lysine specific demethylase-1 (LSD1) inhibitors: A

promising anticancer agents, *Bioorganic Chemistry*, **126**, 105885 **(2022)**

15. Truong T.T., Nguyen P.D., Nguyen N.H., Le T.T.T. and Nguyen T.N., Density functional theory studies on molecular structure, vibrational spectra, AIM, HOMO-LUMO, electronic properties and NBO analysis of benzoic acid monomer and dimer, Ministry of Science and Technology, Vietnam, *Vietnam Journal of Science, Technology and Engineering*, **65(2)**, 3–9 **(2023)**

16. Vijaya P. and Sankaran K.R., A panoptic computational electrochemical profile of p-isobutylacetophenone-local descriptors complement antifungal activity, *Journal of Chemical and Pharmaceutical Research*, **6(10)**, 32-39 **(2014)**

17. Vijaya P. and Sankaran K.R., A combined experimental and DFT study of novel unsymmetrical azine 2-(4-methoxylbenzylidine)-1-(1-(4-isobutylphenyl) ethylidene) hydrazine, *Spectrochimica Acta Part A: Molecular and Biomolecular Spectroscopy*, **138**, 460-473 **(2015)**

18. Villar J.D.F., Determination of ^{19}F & ^{13}C coupling constants and their use in mono fluoro benzaldehyde derivatives conformational analysis, Proceedings of the 5th Meeting of the Nuclear Magnetic Resonance Users, Angra dos Reis, Brazil, 241–245 **(1995)**

19. Wilkens S.J., Markley J.L., Weinhold F. and Westler W.M., Trans-hydrogen-bond (h2)J(NN) and (h1)J(NH) couplings in the DNA A-T base pair: natural bond orbital analysis, *Journal of the American Chemical Society*, **124(7)**, 1190–1191 **(2002)**

20. Yadav Y., Sharma D., Kaushik K., Kumar V., Jha A., Prasad A.K. and Parmar V.S., Synthetic, structural and anticancer activity evaluation studies on novel pyrazolylnucleosides, *Molecules*, **24(21)**, 3922 **(2019)**.

(Received 28th April 2025, accepted 05th July 2025)